Agricultural and Forest Meteorology 288–289 (2020) 107994

Contents lists available at ScienceDirect

Agricultural and Forest Meteorology

journal homepage: www.elsevier.com/locate/agrformet

Forests buffer thermal fluctuation better than *non-forests*

Hua Lin[a,b,*], Chengyi Tu[c,d], Junyong Fang[e], Beniamino Gioli[f], Benjamin Loubet[g], Carsten Gruening[h], Guoyi Zhou[i], Jason Beringer[j], Jianguo Huang[i], Jiří Dušek[k], Michael Liddell[l], Pauline Buysse[g], Peili Shi[m], Qinghai Song[a,b], Shijie Han[n], Vincenzo Magliulo[o], Yingnian Li[p], John Grace[q]

[a] CAS Key Laboratory of Tropical Forest Ecology, Xishuangbanna Tropical Botanical Garden, Chinese Academy of Sciences, Xishuangbanna, 666303, China
[b] Center of Plant Ecology, Core Botanical Gardens, Chinese Academy of Sciences, Xishuangbanna, 666303, China
[c] School of Ecology and Environmental Science, Yunnan University, Kunming, Yunnan, 650091, China
[d] Department of Environmental Science, Policy, and Management, University of California, Berkeley, CA 94720, USA
[e] Institute of Remote Sensing and Digital Earth, Chinese Academy of Sciences, Beijing, 100101, China
[f] CNR-IBE, Institute of BioEconomy, Firenze, Italy
[g] INRA, UMR INRA, AgroParisTech ECOSYS, Université Paris-Saclay, Versailles, 78026, France
[h] European Commission, Joint Research Centre, Ispra, Italy
[i] Key Laboratory of Vegetation Restoration and Management of Degraded Ecosystems, South China Botanical Garden, Chinese Academy of Sciences, Guangzhou, Guangdong, 510650, China
[j] School of Agriculture and Environment, The University of Western Australia, Crawley, WA, 6009, Australia
[k] Global Change Research Institute AS CR, Brno, Czech Republic
[l] Centre for Tropical Environmental and Sustainability Science, James Cook University, Cairns, Queensland, 4811, Australia
[m] Key Laboratory of Ecosystem Network Observation and Modelling, Institute of Geographic Sciences and Natural Resources Research, Chinese Academy of Sciences, Beijing 100101, China
[n] Henan University, Kaifeng, Henan, 475004, China
[o] CNR-ISAFOM, Via Patacca, 85, Ercolano (Napoli), 80056, Italy
[p] Key Laboratory of Adaptation and Evolution of Plateau Biota, Northwest Institute of Plateau Biology, Chinese Academy of Sciences, Xining, Qinghai, 810001, China
[q] School of Geosciences, the University of Edinburgh, Edinburgh EH9 3FF, The United Kingdom

ARTICLE INFO

Keywords:
Deforestation
Global warming
Extreme temperature
Temperature mitigation
Thermal effects
Vegetation index

ABSTRACT

With the increase in intensity and frequency of extreme climate events, interactions between vegetation and local climate are gaining more and more attention. Both the mean temperature and the temperature fluctuations of vegetation will exert thermal influence on local climate and the life of plants and animals. Many studies have focused on the pattern in the mean canopy surface temperature of vegetation, whereas there is still no systematic study of thermal buffer ability (TBA) of different vegetation types across global biomes. We developed a new method to measure TBA based on the rate of temperature increase, requiring only one radiometer. With this method, we compared TBA of ten vegetation types with contrasting structures, e.g. from grasslands to forests, using data from 133 sites globally. TBA ranged from 5.2 to 21.2 across these sites and biomes. Forests and wetlands buffer thermal fluctuation better than non-forests (grasslands, savannas, and croplands), and the TBA boundary between forests and non-forests was typically around 10. Notably, seriously disturbed and young planted forests displayed a greatly reduced TBA as low as that of non-forests at high latitudes. Canopy height was a primary controller of TBA of forests, while the TBA of grasslands and savannas were mainly determined by energy partition, water availability, and carbon sequestration rates. Our research suggests that both mean values and fluctuations in canopy surface temperature should be considered to predict the risk for plants under extreme events. Protecting mature forests, both at high and low latitudes, is critical to mitigate thermal fluctuation under extreme events.

* Corresponding author.
E-mail address: lh@xtbg.ac.cn (H. Lin).

https://doi.org/10.1016/j.agrformet.2020.107994
Received 24 October 2019; Received in revised form 20 February 2020; Accepted 5 April 2020
Available online 14 May 2020
0168-1923/

Acronyms

TBA	Thermal buffer ability
P	Thermal inertia
K	Thermal conductivity
ρ	Density
c	Specific heat capacity
TRN	Thermal response number
ATI	Apparent thermal inertia
S_{in}	Incoming shortwave radiation
S_{out}	Outgoing shortwave radiation
L_{in}	Incoming longwave radiation
L_{out}	Outgoing longwave radiation
R_n	Net radiation
LE	Latent heat flux
H	Sensible heat flux
G	Soil heat flux
NEE	Net ecosystem exchange
RH	Relative humidity
MAP	Mean annual precipitation
MAT	Mean annual air temperature

1. Introduction

Thermal environment is important for all living organisms, as biochemical, physiological and biogeographic processes are all influenced by temperature (Buckley and Huey, 2016; Li et al., 2013). Climate change has been causing an unprecedented rapid increase in the earth's surface temperature over the past century, and this increase is not equally distributed geographically (IPCC, 2013). Vegetation influences the energy balance of the land surface and thus plays an important role in regulating the extent of climate warming at local and global scales (Kalnay and Cai, 2003; Li et al., 2015; Lim et al., 2008; Peng et al., 2014). Different vegetation types may affect the thermal environment through a complex set of biophysical and biochemical attributes and processes (Abe et al., 2017; Evans et al., 2017), including evapotranspiration, albedo, heat capacity, and roughness (Betts, 2000; Bonan, 2008a; Burakowski et al., 2018; Juang et al., 2007) as well as exchange of greenhouse gases and biogenic volatile organic compounds (Bala et al., 2007). Studies of mean canopy surface temperature have demonstrated that tropical forests have cooling effects and boreal forests have warming effects compared with grasslands or croplands; while the situations with respect to temperate forests are more complex depending on the contributions of evapotranspiration and albedo (Abe et al., 2017; Arora and Montenegro, 2011; Bonan, 2008b; Lee et al., 2011; Li et al., 2015). A warming climate presents an ecological threat not just through changing the mean temperature but also through increasing temperature fluctuations (Rummukainen, 2013). Extreme events are likely to affect ecosystems more dramatically and rapidly than slow increases in mean temperature (Bauerfeind and Fischer, 2014; Thompson et al., 2013; Vasseur et al., 2014).

The contrasting structure and energy partitioning of different vegetation types moderate canopy surface temperature, and thus vegetation types may differ in their buffer ability toward temperature fluctuations. Canopy surface temperature of an ecosystem reflects energy balance in the system, while temperature fluctuation indicates the resistance to environmental thermal force, i.e. Thermal Buffer Ability (TBA). In some cases, we might incorrectly neglect the differences in thermal effects between vegetation types if only the mean canopy surface temperature is considered. For example, suppose the temperature of an object A has a lower TBA than an object B; both of them presented the same mean canopy surface temperature, however they may have quite different extreme temperatures (Fig. 1). Vegetation with higher TBA will experience lower extreme temperatures that may protect organisms and prolong the time they need to adapt to a changing climate (Betts et al., 2018). To better understand the interaction between vegetation and climate around the global, it is necessary to study the pattern of TBA and its impact across biomes.

There are several ways to represent TBA (Aerts et al., 2004; Lin et al., 2017a; Price, 1977). Thermal inertia is a measure of the resistance of a material to a change of temperature, defined by $P = \sqrt{K\rho c}$, where K represents the thermal conductivity, ρ and c are density and specific heat capacity respectively (Kahle et al., 1976). Thermal inertia is an important thermal property of a material, independent of the surface color or structure, and has been widely used to classify rock types, produce geological maps, and to estimate soil moisture (Cousin et al., 2013; Kang et al., 2017; Maltese et al., 2013; Price, 1977; Ramakrishnan et al., 2013; Rani et al., 2018). However, TBA of vegetation is somewhat different from the concept of thermal inertia, partly because the properties expressed in P exclude the turbulent transfer of heat and mass i.e. convection and evapotranspiration which are important in vegetation. Moreover, it is impossible to accurately measure K, ρ and c of vegetation in practice due to the dynamic change of water content in plants. Therefore, thermal inertia cannot be directly used to describe TBA of vegetation. The rate of increase in canopy surface temperature over time is another indicator of thermal buffer ability, whereas it strongly depends on incoming radiation (Aerts et al., 2004). Thermal response number (TRN) follows a similar approach as that of apparent thermal inertia (ATI), using the ratio between net radiation and the resulting canopy surface temperature changes (Lin et al., 2009; Luvall and Holbo, 1989). However, TRN has a strong latitude dependence (Lin et al., 2017a), making it inappropriate to compare vegetation across latitudes.

We devised an alternative approach to calculate TBA that can easily be applied using commonly available data. The outgoing longwave radiation (L_{out}) is a proxy for the canopy surface temperature according to the Stephan-Bolzmann law (Joseph, 1879). We calculated TBA by using the reciprocal of the rate of increase of outgoing longwave radiation (L_{out}) over the incoming shortwave radiation (S_{in}). In this way, one two-component radiometer can be used to measure all the variables needed in TBA simultaneously, and TBA is independent of radiation environment. With the development of ecosystem observation networks, a considerable amount of meteorological and energy flux data from diverse ecosystems has been produced, allowing TBA to be

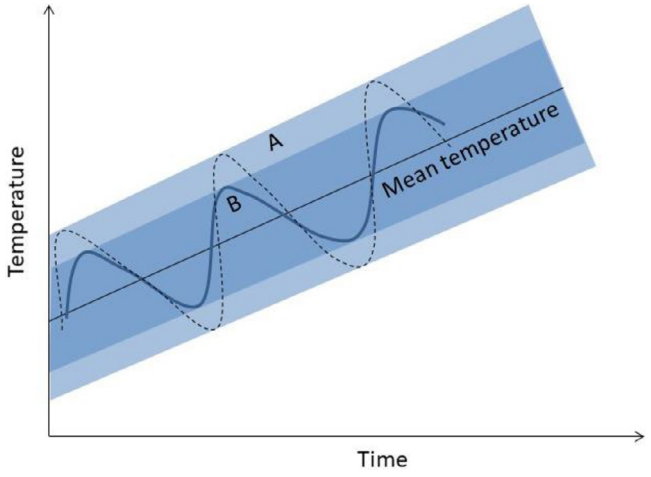

Fig. 1. Temperature change patterns of two objects (A and B) with different TBA under the same radiation environment. The shading area shows the zones of temperature fluctuation of object A (light shading) and B (dark shading) respectively.

obtained for a large range of biomes and conditions. It is also possible to be measured with sensors mounted on a drone. In the present study, ten vegetation types were analyzed to 1) identify the differences in TBA across vegetation types, 2) explore the factors that impact on TBA, and 3) provide suggestions to the vegetation management community on mitigating thermal fluctuation under extreme events.

2. Materials and Methods

2.1. Data sources

Thirty-minute average data were retrieved from the global meteorological and flux monitoring networks: FluxNet, OzFlux (Beringer et al., 2016), and ChinaFlux. Data processing followed the procedures reported on the FLUXNET website http://fluxnet.fluxdata.org/data/fluxnet2015-dataset/data-processing/. All sites providing with four-component radiation data (S_{in}, S_{out}, L_{in}, L_{out}) above the canopy were selected, finally including 133 sites and 10 vegetation types which were classified according to the International Geosphere-Biosphere Programme (IGBP) classes (Fig. 2). Details of the sites can be found in Appendix A.

2.2. The calculation of thermal buffer ability (TBA)

According to the Stefan-Bolzmann law, there is an approximately linear relationship between surface temperature and outgoing longwave radiation (L_{out}) within the temperature range -10 ˚C ~ 45˚C. To simplify the measurement, we used L_{out} instead of surface temperature to calculate the rate of increase of L_{out} over the incoming shortwave radiation (S_{in}), and took its reciprocal as an indicator of TBA (equ. 1). S_{in} was used as a reference to normalize L_{out}, thus TBA is dimensionless. The reference could be L_{in} + S_{in}, net radiation (R_n) or any temperature which can reflect radiation change. TBA calculated using L_{in} + S_{in} or R_n followed similar pattern to the TBA calculated using S_{in} (Appendix B). In practice, S_{in} requires the lowest number of parameters, so we used S_{in} to calculate TBA (equ. 1). This has allowed a two-component radiometer to provide all the required measurements at the same time.

$$TBA = 1/(dL_{out}/dS_{in}) \quad (1)$$

In equation 1, dL_{out}/dS_{in} was the slope of the regression line of L_{out} versus S_{in} when both the two radiation components were increasing. The minimum number of points for the regression was set at four, and only regression lines with an adjusted R-square higher than 0.97 were selected for slope calculation.

2.3. Data analysis

Season division. Following normal meteorological convention, data from June, July and August were used to calculate the summer means, whilst data from December, January and February were used to calculate the winter means in the northern hemisphere. The sites in the southern hemisphere used the opposite seasonal division.

Impact factor analysis. The factors having a potential impact on TBA were investigated using convergent cross mapping (Sugihara et al., 2012; Tu et al., 2019). The basic idea of convergent cross mapping (CCM) is to use prediction between variables as a test for causality. If variable X has a causal effect on variable Y, then causal information of variable X should be present in Y, and so the attractor recovered for variable Y should be able to predict the states of variable X. In practice, the Pearson correlation coefficient between the original time series Y and its estimate from the CCM by another time series X is adopted as a criterion ρ_{ccm}. The larger ρ_{ccm} is, the better X reconstructs Y, and consequently, the stronger the causal effect is (Sugihara et al., 2012). In this work, we are concerned with a more specific problem, distinguishing the driving effects (cause) on variation of TBA from different vegetation types. We used a spatial version of CCM to detect the causality between response variable (result) and the purported drivers (cause, see Table 1). For one possible pair (one purported variable and response variable), we randomly permute the indices of the paired variables, then calculate the correlation of ρ_{ccm}. If correlation of $\rho_{ccm} \rightarrow 1$, then the environmental variable is a driver of TBA; If $\rho_{ccm} \rightarrow 0$, the causality of this pair does not exist. We repeat the shuffling procedure 100 times and test whether the median is significantly larger than zero by Wilcoxon Signed Rank test with correction. A small p-value suggests that it is unlikely that the environmental variable is a driver.

All these analysis were carried out in R 3.6.1.

3. Results

3.1. Comparison of TBA among vegetation types

The global pattern of TBA showed a U shape along absolute latitude with a minimum between absolute latitudes 20˚and 30˚, where main vegetation types were grasslands and savannas. For the present study sites, 78 % of the forests had TBAs more than 10, and 80% of the non-forests (CRO, GRA, OSH, SAV, WET and WSA) had TBA less than 10 in summer (Fig. 3). Generally, TBAs in winter were significantly lower than that in summer (p-value = 0.049). Forests of TBA below 10 were either disturbed, young plantation, or short forests at high latitudes. Wetlands had comparable TBA to forests. A few CRO, SAV, and WSA could have TBA exceeding 10, especially in summer.

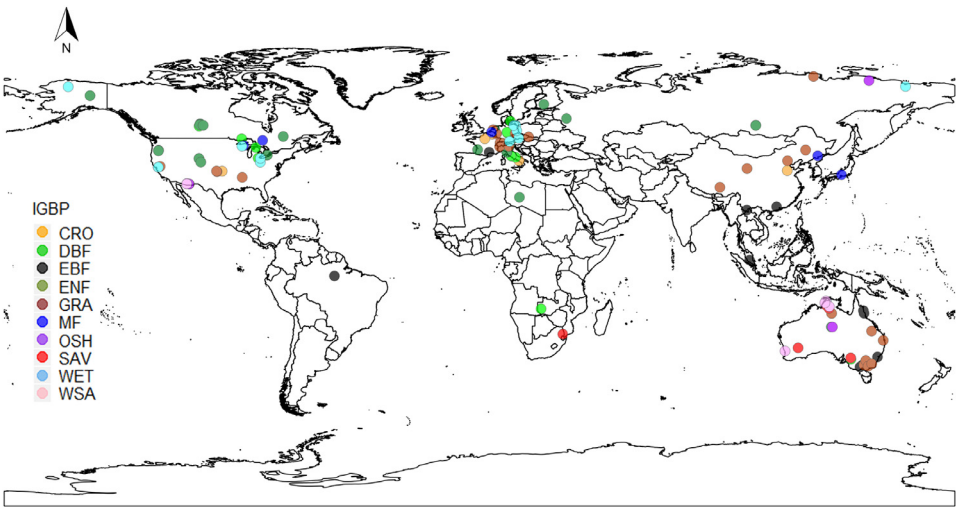

Fig. 2. Distribution of sites. Vegetation types were classified according to International Geosphere-Biosphere Programme (IGBP). CRO, croplands; DBF, deciduous broadleaf forests; EBF, evergreen broadleaf forests; ENF, evergreen needleleaf forests; GRA, grasslands; MF, mixed forests; OSH, open shrublands; SAV, savannas; WET, permanent wetlands; WSA, woody savannas.

Table 1
The variables used for impact factor analysis.

Abbreviation	Full name
G	Mean annual soil heat flux
H	Mean annual sensible heat flux
LE	Mean annual latent heat flux
MAP	Mean annual precipitation
MAT	Mean annual air temperature
NEE	Mean annual net ecosystem exchange
GPP	Mean annual gross primary production
R_n/ S_{in}	The ratio of net radiation to incoming shortwave radiation
RH	Annual mean relative humidity
S_{in}	Mean annual incoming shortwave radiation
B	Bowen ratio, the ratio of *H* to LE

Mature ENF contributed high thermal buffer, while disturbed and young planted ENF had low TBAs close to that of GRA, especially at high latitudes (Fig. 4). Without disturbance, TBA increased with recovery and maturation (Fig. 4 and 5).

3.2. Impact factors on TBA

Different vegetation types had different factors driving TBA. If we mixed all the vegetation types together, we could not find predominant driving factors (e.g. global analysis in fig. 6). For the forests, the most important controlling variable ($\rho_{ccm} > 0.45$) was canopy height, positively related with TBA (Fig. 7a). No strong predictors were found for TBA of CRO and WET. Excluding these two vegetation types from the non-forests (non-forests-2), energy partition between LE and *H*, carbon exchange rate, and water availability were the main variables influencing TBA (Fig. 6). TBA of non-forests-2 exponentially decayed with Bowen ratio, and linearly increased with MAP and RH (Fig. 7 b&6c). The higher net carbon sequestration rate (higher NEE), the higher TBA could be found in non-forests-2 (Fig. 7d). Wind speed had no impact on TBA.

4. Discussion

Our results revealed that forests generally had higher thermal buffer ability (TBA) than non-forests. TBA presented a U shape along absolute latitude until latitude of 60˚. The forests in tropical and temperate zones had high TBA. A TBA "valley" was found between absolute latitude 20˚ - 30˚,the zone dominated by grasslands and savannas. The decline of TBA also occurred at latitudes above 60˚, where almost no natural forests with tall canopy are present. Mature forests were more resistant to environmental temperature change than disturbed and young plantations. Although boreal forests have warming effects compared with

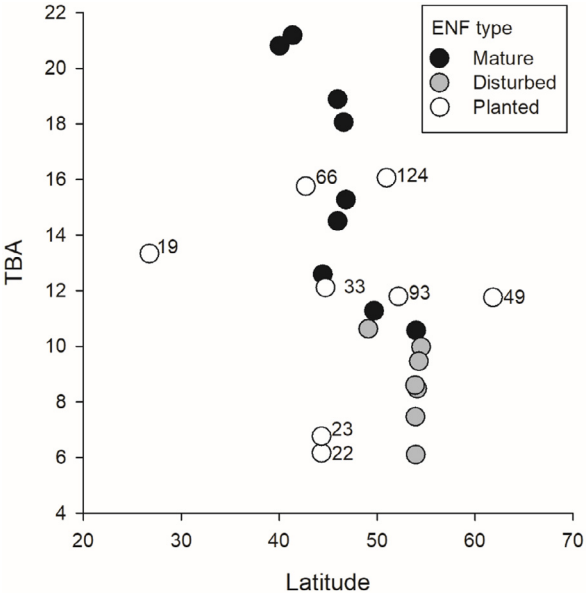

Fig. 4. Comparison of annual mean thermal buffer ability (TBA) among the mature and natural, disturbed, and planted evergreen needleleaf forests (ENF). The age of the planted ENF are given beside the points.

grasslands (Bonan, 2008b; Lee et al., 2011; Li et al., 2015), TBA of boreal forests was higher than grasslands and croplands, except for the degraded forests and young plantations (Frey et al., 2016). Vegetation with high TBA has the potential to moderate local climate under extreme events by minimizing soil evaporation and retaining more water in the ecosystem. During the long-lasting heat-wave events in Europe, forests mitigated the impact of extreme heat, while grasslands accelerated soil moisture depletion and induced high temperatures (Teuling et al., 2010). Specifically, TBA of forests at high latitudes were more susceptible to disturbance than the forests at low latitudes due to short canopy height and simple species composition (Frey et al., 2016; Jucker et al., 2018; Senior et al., 2018). Production-oriented forestry at high latitudes introduced young plantations and aimed to extract wood, which has caused local warming (Naudts et al., 2016). Our results point to possible warming induced by disturbance and plantation and highlight the importance of protecting forests, and in particular reducing disturbance and plantation at high latitudes to mitigate thermal fluctuation under extreme events (Senior et al., 2018). In addition, wetlands are good thermal controllers of the local environment presumably due to the large heat capacity of water. The high thermal buffer abilities of forests and wetlands are expected to mitigate the magnitude of

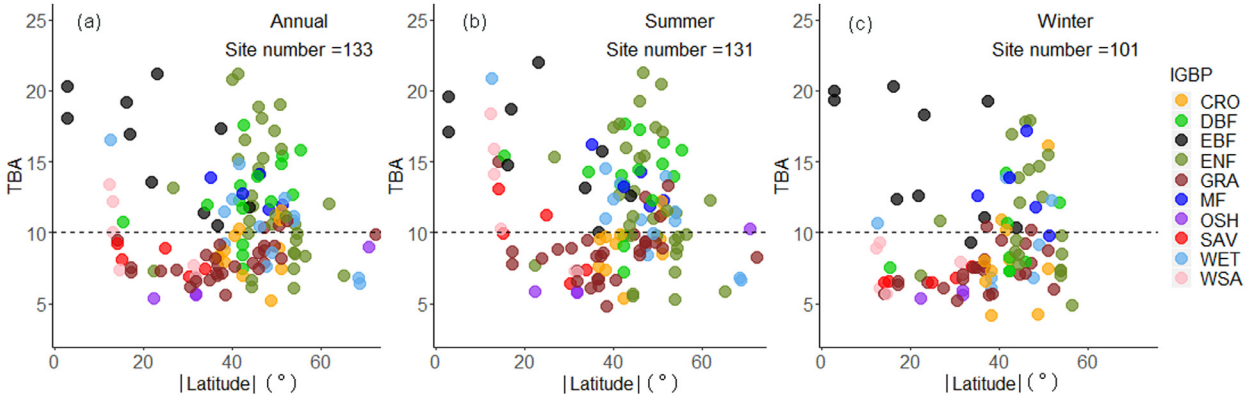

Fig. 3. Thermal buffer ability (TBA) of different vegetation types along latitude (absolute value). Colors were used to distinguish vegetation types (IGBP). CRO, croplands; DBF, deciduous broadleaf forests; EBF, evergreen broadleaf forests; ENF, evergreen needleleaf forests; GRA, grasslands; MF, mixed forests; OSH, open shrublands; SAV, savannas; WET, permanent wetlands; WSA, woody savannas. In total there were 133 sites, but some sites had missing data in summer or winter.

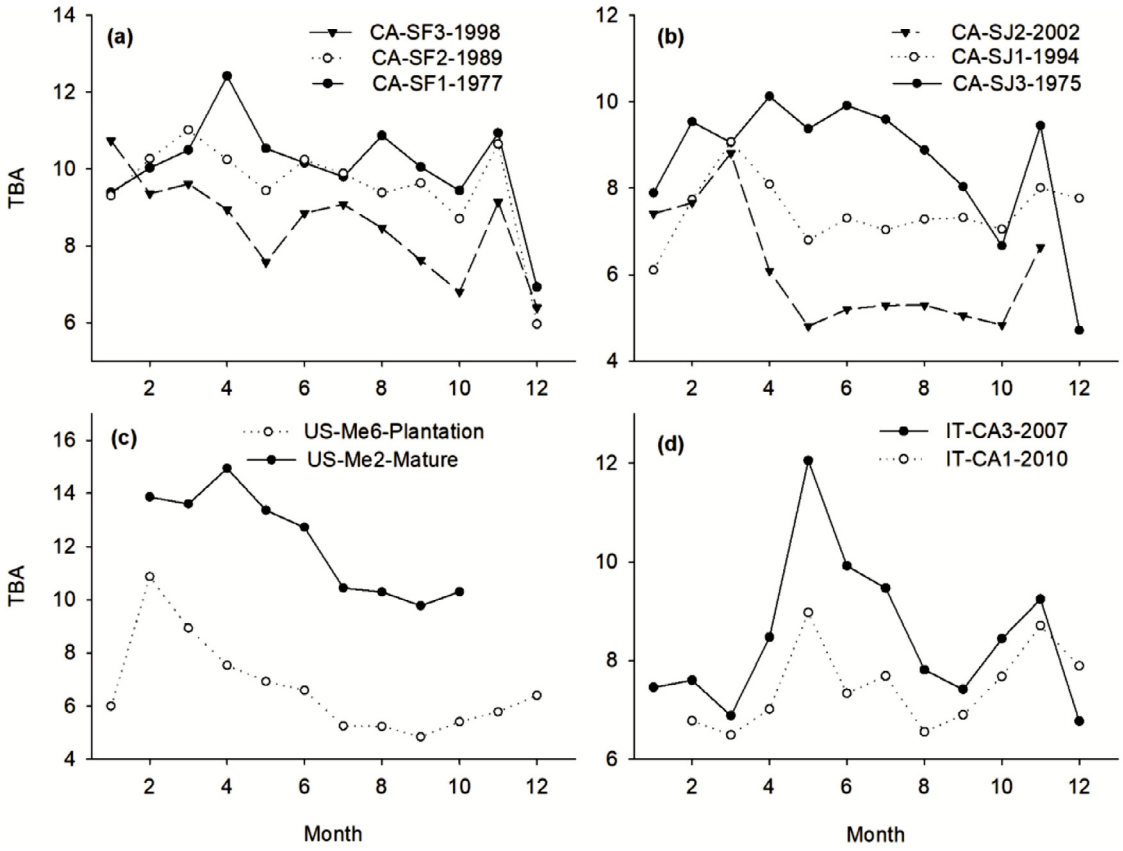

Fig. 5. Comparison of thermal buffer ability (TBA) along forest series. (a). Fire disturbed conifer forests at the site of CA-SF, numbers in the legend indicate the year of disturbance; (b). Harvested conifer forests at the site of CA-SJ, numbers in the legend indicate the harvest year. (c). Pine plantation versus mature pine forest at the site of US-Me; (d). Chronosequences of planted deciduous broadleaf forests at the site of IT-CA, numbers in the legend are the planting year.

extreme events (Diffenbaugh et al., 2017) and provide refuges for the temperature-sensitive species (Betts et al., 2018; Bonan, 2008b). Most biodiversity hot spots are also distributed there (Myers et al., 2000). Unfortunately, a large proportion of forests and wetlands are being transformed into croplands or pastures (Foley et al., 2005). The loss of this high thermal buffer cover across large tracts of land surface has the potential to change both regional and global energy balances, and threaten temperature-sensitive species.

TBA was dependent on physical characteristics and energy exchange of vegetation, whereas the main driving factors were different among vegetation types. For forests, energy exchange, canopy environment and biomass are highly dependent on height. Clear thermal buffer effects of canopy height on microclimate extremes have also been reported in previous studies (Jucker et al., 2018; Lin et al., 2017b; De Frenne et al., 2019). Model simulation and empirical data have revealed that increasing canopy height can amplify surface roughness length, thus facilitating heat exchange (Maes et al., 2011; Raupach, 1994). Meanwhile tall canopy intercepts more sunlight and reduces the heating of solar radiation on ground. The taller forests have more biomass per unit of area, and more biomass in wood. This impacts TBA through the alteration of thermal inertial which is calculated by $P = \sqrt{K\rho c}$. Woods usually have higher K, ρ and c than leaves (Jayalakshmy and Philip, 2010). Accordingly, forests with higher stem biomass should have higher thermal inertia. For the non-forests (excluding croplands and wetlands), the height differences between vegetation types are small, but the hydraulic conditions and water use strategies of plants are divergent from tropical to boreal zones. Evapotranspiration is an efficient way to cool canopy surface temperature. Variations in the Bowen ratio (B) reflect differences in cover, water availability and plant hydraulics, a lower B means more energy is converted to latent heat for evapotranspiration rather than sensible heat. Evapotranspiration is limited by water ability (Redera et al., 2016), TBA was therefore coupled to B, LE, H, MAP and RH. In addition, NEE reflected biomass accumulation and transpiration rate. As reflected in thermal inertia, the vegetation with higher biomass should have higher ρ, and represent higher TBA. Regarding croplands, they are intensively managed and free of water stress, hence we could not find the main driving factors. Although the TBA of wetlands showed a positive relationship with MAT, the sites in the extreme temperature areas were too few to confirm this trend. The impact factor analysis was based on data availability. According to our analysis, it can be concluded that biomass should have a great impact on TBA, however the reliable data is hard to get at a global scale. Further work can explore the relationship between biomass and TBA with remote sensing data, e.g. the planned spatial missions such as Earth Explorer Biomass (Quegan et al., 2019). Albedo was assumed as a main impact factor on mean canopy surface temperature of boreal vegetation (Lee, 2011; Li, 2015), however, we didn't find a significant causality between albedo and TBA. This confirms the point that mean canopy surface temperature and temperature fluctuations have different impact factors, and both of them should be studied to improve our understanding of the interaction between vegetation and climate.

TBA comprehensively reflects energy exchange and physical characteristics of vegetation. It provides a new way to remotely distinguish vegetation properties and monitor vegetation degradation, succession and recovery (Aerts et al., 2004; Lin et al., 2017a). According to our results, TBA of 10 could be used as an indicator of serious forest degradation as it represents a boundary of TBA between forests and non-forests. In a previous study, a vegetation health index (VHI) combining land surface temperature (LST) and normalized difference vegetation index (NDVI) has been proposed (Kogan, 1995). VHI has been used to detect drought (Seiler et al., 1998; Unganai and Kogan, 1998), estimate

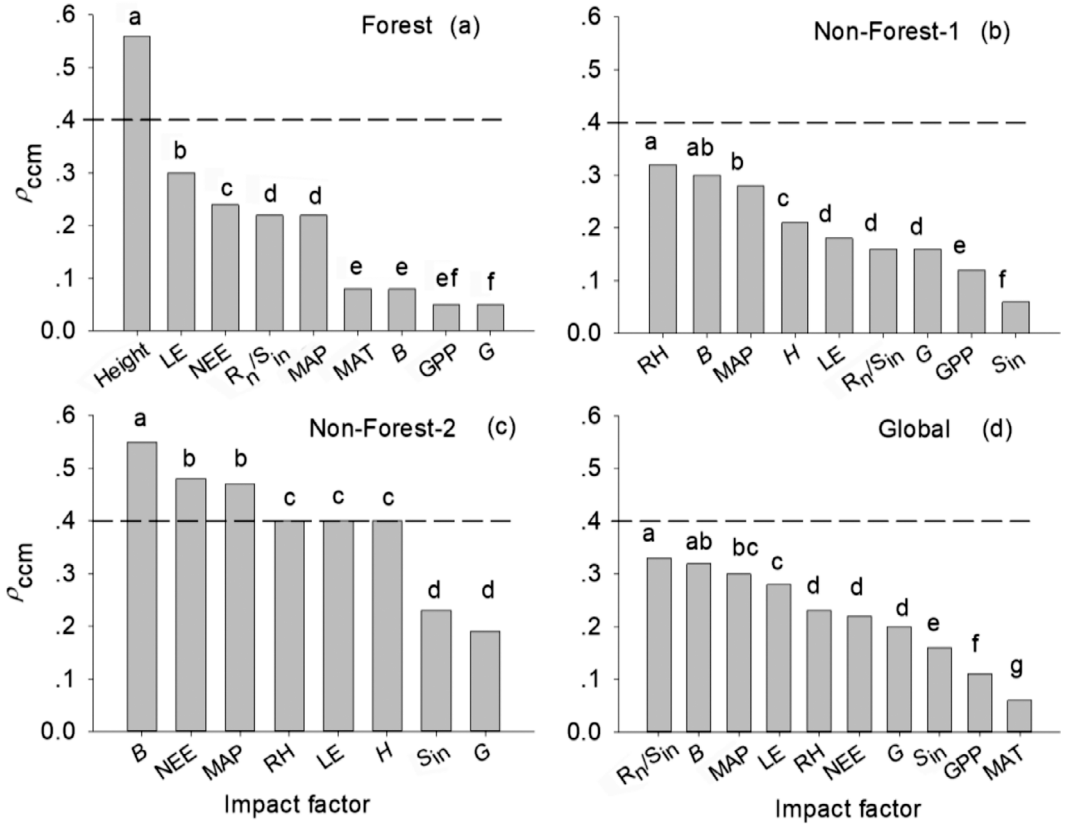

Fig. 6. Causality test of impact factors on TBA for (a) forests, (b) non-forests-1, (c) non-forests-2 and (d) global vegetation. ρ_{ccm} represents the strength of causality; Forests include deciduous broadleaf forests, evergreen needleleaf forests, and mixed forests; Non-forests-1 includes croplands, grasslands, open shrublands, permanent wetlands, savannas and woody savannas; Non-forests-2 excludes croplands and permanent wetlands from non-forests-1. Height, canopy height, no canopy height data for non-forests; R_n/S_{in}, the ratio of net radiation to incoming shortwave radiation; GPP, mean annual gross primary production; NEE, mean annual net ecosystem exchange; LE, mean annual latent heat flux; *H*, mean annual sensible heat flux; *G*, mean annual soil heat flux; *B*, mean annual Bowen ratio; MAT, mean annual air temperature; MAP, mean annual precipitation.

vegetation density, and calculate biomass (Gitelson et al., 1998). However, canopy surface temperature strongly depends on the instantaneous radiation environment, making it incomparable under different radiation conditions. In contrast, TBA was not influenced by wind speed and used the incoming solar radiation as a reference, which normalized canopy surface temperature to the same radiation environment. In this way, it solves both the temporal limitation of VHI and the spatial limitation of TRN in practice. With the development of thermal remote sensing and drone technology, the application of TBA will become more and more convenient in the future.

5. Conclusions

The large scale patterns and the impact factors driving temperature fluctuation (represented by TBA) are different from the pattern and driving factors of mean canopy surface temperature of vegetation. Although the mature conifer forests at high latitudes induce warming effects, their TBA are higher than non-forests. They are of important ecological significance to mitigate local thermal fluctuation under extreme thermal events. The threshold of TBA between forests and non-forests is around 10. This TBA value then can be used as an indicator of forest degradation. Disturbances that destroy canopy height can significantly reduce TBA, especially for the forests at high latitudes. Bowen ratio, water availability, and carbon sequestration rates are the main impact factors on TBA of non-forests such as grasslands and savannas.

This study suggests that reliable estimates of TBA globally will improve our understanding of the interaction between vegetation and climate and help land managers evaluate the risk of plants and animals under extreme events (Thompson et al., 2013). Our study demonstrates that forest degradation and deforestation reduce TBA. Globally monitoring TBA becomes an important element to track and protect high TBA vegetation to provide thermal buffering for biodiversity to resist climate change.

Declaration of Competing Interest

The authors declare that they have no known competing financial interests or personal relationships that could have appeared to influence the work reported in this paper

Acknowledgements

This research was funded by the National Natural Science Foundation of China (grant number 31870386), the CAS 135 Program (grant number 2017XTBG-F01), Open Fund of State Key Laboratory of Remote Sensing Science (grant number OFSLRSS201805), Open Fund of Key Laboratory of Tropical Forest Ecology, Xishuangbanna Tropical Botanical Garden, Chinese Academy of Sciences (grant number 09KF001B04) and the National Natural Science Foundation of China (NSCF-TRF project, grant number 4186114401). This work used eddy covariance data acquired and shared by the FLUXNET community, including the networks: AmeriFlux, AfriFlux, AsiaFlux, CarboAfrica, CarboEuropeIP, CarboItaly, CarboMont, ChinaFlux, Fluxnet-Canada, GreenGrass, ICOS, KoFlux, LBA, NECC, TERN OzFlux, TCOS-Siberia, and USCCC. The ERA-Interim reanalysis data were provided by ECMWF and processed by LSCE. The FLUXNET eddy covariance data processing

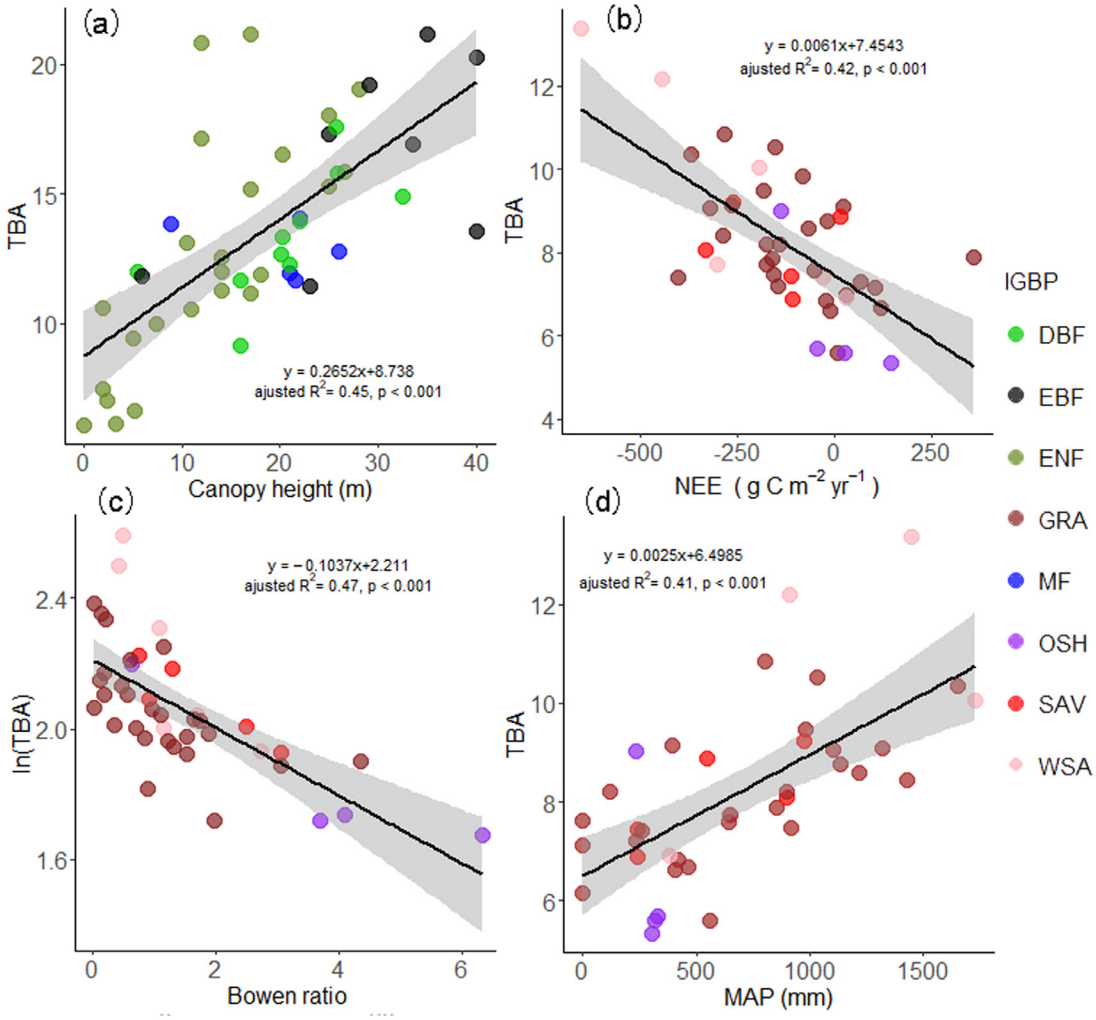

Fig. 7. The relationship between thermal buffer ability (TBA) and its main driving factors. NEE, mean annual net ecosystem exchange; MAP, mean annual precipitation. Shading area shows the confidence interval of 0.95; Bowen ratio, the ratio of sensible heat to latent heat.

and harmonization was carried out by the European Fluxes Database Cluster, AmeriFlux Management Project, and Fluxdata project of FLUXNET, with the support of CDIAC and ICOS Ecosystem Thematic Center, Council for Scientific and Industrial Research (CSIR), and the OzFlux, ChinaFlux and AsiaFlux offices. Support for collection and archiving of Ozflux data was provided through the Australia Terrestrial Ecosystem Research Network (TERN) (http://www.tern.org.au). Thanks to Professor Patrick Finnegan for the comments on the manuscript.

Appendix

A. Site information.

No	Site	Latitude (°)	Longitude (°)	IGBP	Canopy height (m)	Year	Status
1	AT-Neu	47.11667	11.3175	GRA		2006-2012	
2	AU-Ade	-13.0769	131.1178	WSA		2007-2009	
3	AU-ASM	-22.283	133.249	ENF		2010-2014	
4	AU-Cpr	-34.0027	140.5877	SAV		2010-2014	
5	AU-Cum	-33.6153	150.7236	EBF	23	2012-2014	
6	AU-DaP	-14.0633	131.3181	GRA		2017-2013	
7	AU-DaS	-14.1592	131.3881	SAV		2008-2014	
8	AU-Dry	-15.2588	132.3706	SAV		2008-2014	
9	AU-Emr	-23.8587	148.4746	GRA		2011-2013	
10	AU-Fog	-12.5425	131.307	WET		2006-2008	
11	AU-Gin	-31.3764	115.7139	WSA		2011-2014	
12	AU-GWW	-30.1913	120.6541	SAV		2013-2014	
13	AU-How	-12.4943	131.152	WSA		06-08, 10-11, 13-14	
14	AU-Lox	-34.4704	140.6551	DBF	5.5	2008-2009	Planted
15	AU-RDF	-14.5636	132.4776	WSA		2011-2013	
16	AU-Rig	-36.6499	145.576	GRA		2011-2014	

17	AU-Rob	-17.1175	145.6301	EBF	33.5	2014	Mature
18	AU-Stp	-17.1507	133.3502	GRA		2008-2014	
19	AU-TTE	-22.287	133.64	OSH		2012-2014	
20	AU-Whr	-36.6732	145.0294	EBF		2011-2014	
21	AU-Wom	-37.4222	144.0944	EBF	25	2010-2014	Disturbed
22	AU-Ync	-34.9893	146.2907	GRA		2012-2014	
23	BE-Bra	51.3092	4.52056	MF	21	2007-2014	Planted
24	BE-Lon	50.5522	4.74494	CRO		2005-2007, 2009-2014	
25	BR-Sa3	-3.018	-54.9714	EBF	40	2001-2003	Disturbed
26	CA-Gro	48.2167	-82.1556	MF	21.6	2004-2014	
27	CA-Oas	53.6289	-106.198	DBF	20.1	1996-2010	Mature
28	CA-Obs	53.9872	-105.118	ENF	11	1997-2010	Mature
29	CA-Qfo	49.6925	-74.3421	ENF	14	2004-2010	Mature
30	CA-SF1	54.485	-105.818	ENF	7.4	2004-2005	1977 burnt
31	CA-SF2	54.2539	-105.878	ENF	5	2004-2005	1989 burnt
32	CA-SF3	54.0916	-106.005	ENF		2004-2005	1998 burnt
33	CA-SJ1	53.908	-104.656	ENF	2	2004-2005	1994 harvest
34	CA-SJ2	53.94474	104.6493	ENF	0.1	2004-2005	2002 harvest
35	CA-SJ3	53.87581	104.6453	ENF		2004-2005	1975 harvest
36	CA-TP4	42.7098	-80.3574	ENF	20.2	2003-2014	1939 Planted
37	CA-TPD	42.63531	-80.5576	DBF	25.7	2012-2014	Mature
38	CH-Cha	47.21022	8.410444	GRA		2006-2012	
39	CH-Dav	46.8153	9.8559	ENF	25	2007-2011	Mature
40	CH-Fru	47.11583	8.537778	GRA		2006-2012	
41	CH-Oe1	47.2856	7.73214	GRA		2003-2008	
42	CN-Cng	44.5934	123.5092	GRA		2007-2010	
43	CZ-BK1	49.50213	18.53686	ENF	12	2006-2007, 2009-2014	
44	CZ-BK2	49.4944	18.5429	GRA		2006-2012	
45	CZ-wet	49.02465	14.77035	WET		2006-2012	
46	DE-Akm	53.86617	13.68342	WET		2010-2014	
47	DE-Geb	51.1001	10.9143	CRO		2001-2014	
48	DE-Gri	50.9495	13.5125	GRA		2007-2014	
49	DE-Hai	51.0793	10.452	DBF	32.5	2003-2012	Mature
50	DE-Kli	50.8929	13.5225	CRO		2004-2014	
51	DE-Lkb	49.0996	13.3047	ENF	2	2009-2011, 2013	2007 disturbed
52	DE-Lnf	51.32822	10.3678	DBF		2002-2006, 2010-2012	
53	DE-Obe	50.78362	13.71963	ENF	28	2008-2014	
54	DE-RuR	50.62191	6.304126	GRA		2011-2014	
55	DE-RuS	50.8659	6.4472	CRO		2011-2014	
56	DE-SfN	47.80639	11.3275	WET		2012-2014	
57	DE-Spw	51.89225	14.03369	WET		2010-2014	
58	DE-Tha	50.9636	13.5669	ENF	26.5	2004-2006, 2008-2014	1887 planted
59	DE-Zrk	53.87594	12.88901	WET		2013	
60	DK-Sor	55.48587	11.64464	DBF	25.8	2006, 2008-2013	
61	FI-Hyy	61.8474	24.2948	ENF	14	2010-2014	1962 planted
62	FR-Gri	48.8442	1.9519	CRO		2007-2008	
63	FR-LBr	44.7171	-0.7693	ENF	18	2003-2008	1972 planted
64	FR-Pue	43.7414	3.59583	EBF	6	2005-2014	Disturbed
65	IT-BCi	40.5238	14.9574	CRO		2006-2010	
66	IT-CA1	42.3804	12.0266	DBF		2011-2014	2010 planted
67	IT-CA2	42.3772	12.026	CRO		2012-2014	
68	IT-CA3	42.38	12.0222	DBF		2012-2014	2007 planted
69	IT-Col	41.8494	13.5881	DBF	20.2	2005-2014	
70	IT-Isp	45.81264	8.633579	DBF		2013-2014	Planted
71	IT-La2	45.9542	11.2853	ENF		2000-2001	Mature
72	IT-Lav	45.9553	11.2812	ENF		2003-2014	Mature
73	IT-MBo	46.0156	11.0467	GRA		2003-2013	
74	IT-Noe	40.6062	8.1512	CSH		04, 08, 09,12	
75	IT-Ren	46.5878	11.4347	ENF	25	2004, 2006-2013	Mature
76	IT-Ro1	42.4081	11.93	DBF	16	2005-2006	Disturbed
77	IT-Ro2	42.3903	11.9209	DBF	16	2010	Disturbed
78	IT-SR2	43.73203	10.29095	ENF		2013-2014	
79	IT-SRo	43.72786	10.28444	ENF		2004-2007	
80	IT-Tor	45.8444	7.5781	GRA		2008-2014	
81	JP-SMF	35.2617	137.0788	MF	8.9	2003-2005	
82	MY-PSO	2.973	102.3062	EBF		2003-2005, 2007-2009	Mature
83	NL-Hor	52.24035	5.071301	GRA		2004-2011	
84	NL-Loo	52.1679	5.74396	ENF	17	1999-2000, 2002-2014	1909 planted
85	RU-Che	68.613	161.3414	WET		2008, 2011-2014	
86	RU-Cok	70.8291	147.4943	OSH		2003-2014	
87	RU-Fyo	56.46153	32.92208	ENF		1998-2014	
88	RU-Sam	72.3738	126.4958	GRA		2002, 2005, 2013	
89	RU-SkP	62.255	129.168	DNF		2012-2014	
90	US-AR1	36.4267	-99.42	GRA		2009-2012	
91	US-AR2	36.6358	-99.5975	GRA		2009-2012	
92	US-ARM	36.6058	-97.4888	CRO		2003-2012	
93	US-CRT	41.6285	-83.3471	CRO		2011-2013	
94	US-GBT	41.3658	-106.24	ENF	17	2000-2002, 2005-2006	
95	US-GLE	41.3644	-106.239	ENF	17	2005-2014	Mature
96	US-Goo	34.2547	-89.8735	GRA		2002-2006	

97	US-Ivo	68.4865	-155.75	WET		2004-2005	
98	US-Los	46.0827	-89.9792	WET		2014	
99	US-Me2	44.4523	-121.557	ENF	14	2010-2014	Mature
100	US-Me3	44.3154	-121.608	ENF	3.3	2009	1987 planted
101	US-Me6	44.3232	-121.604	ENF	5.2	2010-2014	1990 planted
102	US-NR1	40.0329	-105.546	ENF	12	2001, 2006-2014	Mature
103	US-Oho	41.5545	-83.8438	DBF	21	2004-2013	Disturbed
104	US-ORv	40.0201	-83.0183	WET		2011	
105	US-Prr	65.1247	-147.488	ENF	2.44	2011-2014	
106	US-SRC	31.90831	-110.839	OSH		2008-2014	
107	US-SRG	31.7894	-110.828	GRA		2008-2014	
108	US-SRM	31.8214	-110.866	WSA		2004-2014	
109	US-Syv	46.242	-89.3477	MF	22	2012-2014	Mature
110	US-Tw1	38.1074	-121.647	WET		2012-2014	
111	US-Tw2	38.1047	-121.643	CRO		2012-2013	
112	US-Tw3	38.1159	-121.647	CRO		2013-2014	
113	US-Tw4	38.103	-121.641	WET		2013-2014	
114	US-UMd	45.5598	-84.7138	DBF	22	2010, 2012-2014	Disturbed
115	US-Var	38.4133	-120.951	GRA		2004-2014	
116	US-WCr	48.8059	-90.0799	DBF		1999-2006, 2014	Disturbed
117	US-Whs	31.74383	-110.052	OSH		2009-2014	
118	US-Wkg	31.7365	-109.942	GRA		2004-2014	
119	US-WPT	41.4646	-82.9962	WET		2011-2013	
120	ZA-Kru	-25.0197	31.4969	SAV		2000-2003	
121	ZM-Mon	-15.4378	23.25278	DBF		2007-2009	Disturbed
122	CN-cbs	42.4025	128.0958	MF	26	2003-2007	Mature
123	CN-dhs	23.16667	112.5167	EBF	35	2003-2007	Mature
124	CN-dxg	30.49728	91.06636	GRA		2003-2007	
125	CN-hgc	37.61277	101.3312	GRA		2003-2007	
126	CN-nmg	40.53333	116.6667	GRA		2003-2007	
127	CN-qyz	26.7414	15.0581	ENF	10.5	2003-2007	1985 planted
128	CN-xbn	21.9275	101.2653	EBF	40	2003-2007	Mature
129	CN-yca	36.8333	116.5666	CRO		2003-2007	
130	AU-Ctr	-16.1056	145.3778	EBF	29	2012, 2014-2015	Mature
131	AU-Drg	-37.1334	147.171	GRA		2007-2013	
132	AU-Lit	-13.179	130.7945	WSA		2015-2016	
133	AU-Nim	-36.2159	148.5525	GRA		2008-2013	

CRO, croplands; DBF, deciduous broadleaf forests; EBF, evergreen broadleaf forests; ENF, evergreen needleleaf forests; GRA, grasslands; MF, mixed forests; OSH, open shrublands; SAV, savannas; WET, permanent wetlands; WSA, woody savannas. Only the forests statuses with known status were given.

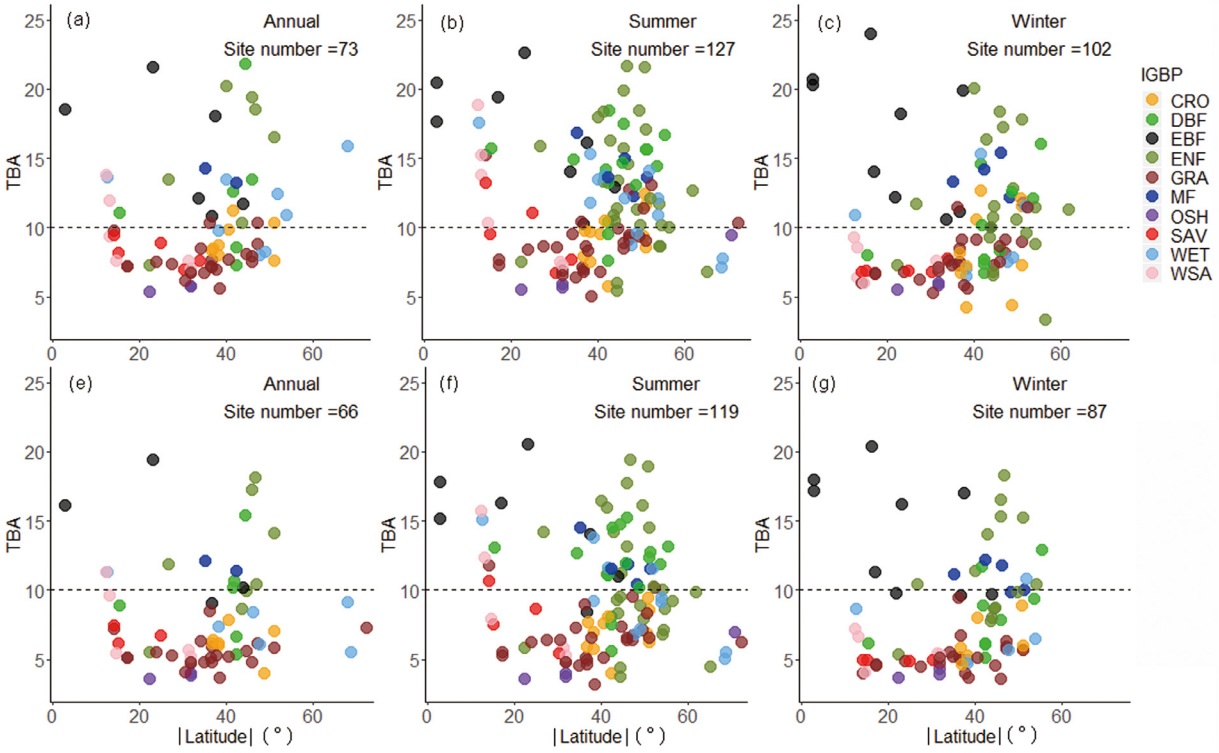

B. Thermal buffer ability (TBA) calculated by incoming shortwave radiation + incoming longwave radiation (L_{in} + S_{in}) (a-c), and by net radiation (R_n) (e-g). CRO, croplands; DBF, deciduous broadleaf forests; EBF, evergreen broadleaf forests; ENF, evergreen needleleaf forests; GRA, grasslands; MF, mixed forests; OSH, open shrublands; SAV, savannas; WET, permanent wetlands; WSA, woody savannas. Latitudes are in absolute value.

Supplementary materials

Supplementary material associated with this article can be found, in the online version, at doi:10.1016/j.agrformet.2020.107994.

References

Abe, M., Takata, K., Kawamiya, M., Watanabe, S., 2017. Vegetation masking effect on future warming and snow albedo feedback in a boreal forest region of northern Eurasia according to MIROC-ESM. J. Geophys. Res.-Atmos. 122 (17), 9245–9261.

Aerts, R., et al., 2004. . Ecosystem thermal buffer capacity as an indicator of the restoration status of protected areas in the northern Ethiopian highlands. Restoration Ecology 12 (4), 586–596.

Arora, V.K., Montenegro, A., 2011. Small temperature benefits provided by realistic afforestation efforts. Nature Geosci 4 (8), 514–518.

Bala, G., et al., 2007. . Combined climate and carbon-cycle effects of large-scale deforestation. Proc. Natl. Acad. Sci. U. S. A. 104 (16), 6550–6555.

Bauerfeind, S.S., Fischer, K., 2014. Simulating climate change: temperature extremes but not means diminish performance in a widespread butterfly. Popul. Ecol. 56 (1), 239–250.

Beringer, J., et al., 2016. An introduction to the Australian and New Zealand flux tower network - OzFlux. Biogeosciences 13 (21), 5895–5916.

Betts, M.G., Phalan, B., Frey, S.J.K., Rousseau, J.S., Yang, Z.Q., 2018. Old-growth forests buffer climate-sensitive bird populations from warming. Divers. Distrib. 24 (4), 439–447.

Betts, R.A., 2000. Offset of the potential carbon sink from boreal forestation by decreases in surface albedo. Nature 408 (6809), 187–190.

Bonan, G.B., 2008a. Ecological climatology: concepts and applications. Cambridge University Press, Cambridge; New York xvi, 550 p. pp.

Bonan, G.B., 2008b. Forests and climate change: Forcings, feedbacks, and the climate benefits of forests. Science 320 (5882), 1444–1449.

Buckley, L.B., Huey, R.B., 2016. How extreme temperatures impact organisms and the evolution of their thermal tolerance. Integr. Comp. Biol. 56. E27–E27.

Burakowski, E., et al., 2018. The role of surface roughness, albedo, and Bowen ratio on ecosystem energy balance in the Eastern United States. Agric. For. Meteorol. 249, 367–376.

Cousin, I., Pasquier, C., Seger, M., Tabbagh, A., 2013. Using airborne thermal inertia mapping to analyze the soil spatial variability at regional scale. In: Globalsoilmap: Basis of the Global Spatial Soil Information System: Proceedings of the 1rst Global soilmapconferenc. CRC Press Taylor & Francis Group, pp. 441–446.

De Frenne, P., et al., 2019. Global buffering of temperatures under forest canopies. Nat. Ecol. Evol. 3, 744–749.

Diffenbaugh, N.S., et al., 2017. Quantifying the influence of global warming on unprecedented extreme climate events. Proc. Natl. Acad. Sci. U. S. A. 114 (19), 4881–4886.

Evans, J.P., Meng, X.H., McCabe, M.F., 2017. Land surface albedo and vegetation feedbacks enhanced the millennium drought in south-east Australia. Hydrol. Earth Syst. Sc. 21 (1), 409–422.

Foley, J.A., et al., 2005. Global consequences of land use. Science 309 (5734), 570–574.

Frey, S.J.K., et al., 2016. Spatial models reveal the microclimatic buffering capacity of old-growth forests. Sci. Adv. 2 (4), e1501392.

Gitelson, A.A., Kogan, F., Zakarin, E., Spivak, L., Lebed, L., 1998. Using AVHRR data for quantitive estimation of vegetation conditions: Calibration and validation. Adv. Space Res. 22 (5), 673–676.

IPCC, 2013. Climate change 2007: The physical science basis. Cambridge University Press, Cambridge.

Jayalakshmy, M.S., Philip, J., 2010. Thermophysical properties of plant leaves and their influence on the environment temperature. International Journal of Thermophysics 31, 2295–2304.

Joseph, S., 1879. Über die beziehung zwischen der Wärmestrahlung und der Temperatur. Sitzungsberichte der Kaiserlichen Akademie der Wissenschaften. Mathematisch-naturwissenschaftliche Classe 79, 391–428.

Juang, J.Y., Katul, G., Siqueira, M., Stoy, P., Novick, K., 2007. Separating the effects of albedo from eco-physiological changes on surface temperature along a successional chronosequence in the southeastern United States. Geophys. Res. Lett. 34 (21), L21408.

Jucker, T., et al., 2018. Canopy structure and topography jointly constrain the microclimate of human-modified tropical landscapes. Global Change Biol 24 (11), 5243–5258.

Kahle, A.B., Gillespie, A.R., Goetz, A.F.H., 1976. Thermal inertia imaging - new geologic mapping tool. Geophys. Res. Lett 3 (1), 26–28.

Kalnay, E., Cai, M., 2003. Impact of urbanization and land-use change on climate. Nature 423 (6939), 528–531.

Kang, J., et al., 2017. High spatio-temporal resolution mapping of soil moisture by integrating wireless sensor network observations and MODIS apparent thermal inertia in the Babao River Basin, China. Remote Sens. Environ. 191, 232–245.

Kogan, F.N., 1995. Application of vegetation index and brightness temperature for drought detection. Adv. Space Res. 15 (11), 91–100.

Lee, X., et al., 2011. Observed increase in local cooling effect of deforestation at higher latitudes. Nature 479 (7373), 384–387.

Li, F., et al., 2013. Temperature change and macroinvertebrate biodiversity: assessments of organism vulnerability and potential distributions. Clim. Change 119 (2), 421–434.

Li, Y., et al., 2015. Local cooling and warming effects of forests based on satellite observations. Nat Commun 6, 6603.

Lim, Y.K., Cai, M., Kalnay, E., Zhou, L., 2008. Impact of vegetation types on surface temperature change. J. Appl. Meteorol. Clim. 47 (2), 411–424.

Lin, H., Cao, M., Stoy, P.C., Zhang, Y.P., 2009. Assessing self-organization of plant communities-A thermodynamic approach. Ecol. Model. 220 (6), 784–790.

Lin, H., et al., 2017a. . Quantifying deforestation and forest degradation with thermal response. Sci. Total Environ. 607, 1286–1292.

Lin, H., et al., 2017b. . The cooling trend of canopy temperature during the maturation, succession, and recovery of ecosystems. Ecosystems 20 (2), 406–415.

Luvall, J.C., Holbo, H.R., 1989. Measurements of Short-Term Thermal Responses of Coniferous Forest Canopies Using Thermal Scanner Data. Remote Sens. Environ. 27 (1), 1–10.

Maes, W.H., Pashuysen, T., Trabucco, A., Veroustraete, F., Muys, B., 2011. Does energy dissipation increase with ecosystem succession? Testing the ecosystem exergy theory combining theoretical simulations and thermal remote sensing observations. Ecol. Model 222 (23-24), 3917–3941.

Maltese, A., Capodici, F., La Loggia, G., Corbari, C. and Mancini, M., 2013. A validation of a thermal inertia approach to map soil water content on soils characterized by low fractional cover, Remote Sensing for Agriculture, Ecosystems, and Hydrology Xv, Dresden, Germany.

Myers, N., Mittermeier, R.A., Mittermeier, G.G., Fonseca, G.A.B.d., Kent, J., 2000. Biodiversity hotspots for conservation priorities. Nature 403 (24), 854–858.

Naudts, K., et al., 2016. Europe's forest management did not mitigate climate warming. Science 351 (6273), 597–600.

Peng, S.S., et al., 2014. Afforestation in China cools local land surface temperature. Proc. Natl. Acad. Sci. U. S. A. 111 (8), 2915–2919.

Price, J.C., 1977. Thermal Inertia Mapping - New View of Earth. J Geophys Res-Oc Atm 82 (18), 2582–2590.

Ramakrishnan, D., Bharti, R., Singh, K.D., Nithya, M., 2013. Thermal inertia mapping and its application in mineral exploration: results from Mamandur polymetal prospect. India. Geophys. J. Int 195 (1), 357–368.

Rani, K., Guha, A., Pal, S.K., 2018. Satellite-derived regional apparent thermal inertia and gravity for mapping different rock types in parts of banswara, rajasthan. J. Geol. Soc. India 92 (6), 671–678.

Raupach, M.R., 1994. Simplified expressions for vegetation roughness length and zero-plane displacement as functions of canopy height and area index. Boundary-Layer Meteorology 71 (1-2), 211–216.

Redera, A., Rianna, G. and Pagano, L., 2016. Evaluation of the effect of land vegetation cover on water and energy balance of an unsaturated pyroclastic cover. E3s Web Conf, 9.

Rummukainen, M., 2013. Climate change: changing means and changing extremes. Clim. Change 121 (1), 3–13.

Seiler, R.A., Kogan, F., Sullivan, J., 1998. AVHRR-based vegetation and temperature condition indices for drought detection in Argentina. Adv. Space Res. 21 (3), 481–484.

Senior, R.A., Hill, J.K., Benedick, S., Edwards, D.P., 2018. Tropical forests are thermally buffered despite intensive selective logging. Global Change Biol 24 (3), 1267–1278.

Sugihara, G., et al., 2012. Detecting causality in complex ecosystems. Science 338 (6106), 496–500.

Teuling, A.J., et al., 2010. Contrasting response of European forest and grassland energy exchange to heatwaves. Nat Geosci 3 (10), 722–727.

Thompson, R.M., Beardall, J., Beringer, J., Grace, M., Sardina, P., 2013. Means and extremes: building variability into community-level climate change experiments. Ecol. Lett. 16 (6), 799–806.

Tu, C., Fan, Y., Fan, J., 2019. Universal cointegration and its applications. iSicence 19, 986–995.

Unganai, L.S., Kogan, F.N., 1998. Southern Africa's recent droughts from space. Adv. Space Res. 21 (3), 507–511.

Vasseur, D.A., et al., 2014. Increased temperature variation poses a greater risk to species than climate warming. P. Roy. Soc. B-Biol. Sci. 281 (1779), 20132612.